Eur. Phys. J. Spec. Top.
https://doi.org/10.1140/epjs/s11734-025-01503-4

THE EUROPEAN PHYSICAL JOURNAL SPECIAL TOPICS

Review

Radio detection of ultrahigh-energy cosmic-ray air showers

Frank G. Schröder[1,2,a]

[1] Department of Physics and Astronomy, Bartol Research Institute, University of Delaware, Sharp Lab, 104 The Green, Newark, DE 19716, USA
[2] Institute for Astroparticle Physics, Karlsruhe Institute of Technology (KIT), Hermann-von-Helmholtz-Platz 1, 76344 Eggenstein-Leopoldshafen, Germany

Received 6 September 2024 / Accepted 29 January 2025

Abstract Radio antennas have become a standard tool for the detection of cosmic-ray air showers in the energy range above 10^{16} eV. The radio signal of these air showers is generated mostly due to the deflection of electrons and positrons in the geomagnetic field, and contains information about the energy and the depth of the maximum of the air showers. Unlike the traditional air-Cherenkov and air-fluorescence techniques for the electromagnetic shower component, radio detection is not restricted to clear nights, and recent experiments have demonstrated that the measurement accuracy can compete with these traditional techniques. Numerous particle detector arrays for air showers have thus been or will be complemented by radio antennas. In particular when combined with muon detectors, the complementary information provided by the radio antennas can enhance the total accuracy for the arrival direction, energy and mass of the primary cosmic rays. Digitization and computational techniques have been crucial for this recent progress, and radio detection will play an important role in next-generation experiments for ultrahigh-energy cosmic rays. Moreover, stand-alone radio experiments are under development and will search for ultrahigh-energy photons and neutrinos in addition to cosmic rays. This article provides a brief introduction to the physics of the radio emission of air showers, an overview of air-shower observatories using radio antennas, and highlights some of their recent results.

Abbreviations

AERA	Auger Engineering Radio Array
ANITA	ANtarctic Impulsive Transient Antenna
ARA	Askaryan Radio Array
ARIANNA	Antarctic Ross Ice-Shelf Antenna Neutrino Array
Auger	Pierre Auger Observatory
BEACON	Beamforming Elevated Array for COsmic Neutrinos
CODALEMA	COsmic ray Detection Array with Logarithmic ElectroMagnetic Antennas
GCOS	Global Cosmic-Ray Observatory
GRAND	Giant Radio Array for Neutrino Detection
IceCube-Gen2	IceCube Neutrino Observatory-Generation 2
LOFAR	LOw-Frequency ARray
LOPES	LOFAR PrototypE Station
OVRO	Owens Valley Radio Observatory
PBR	POEMMA-Balloon with Radio
POEMMA	Probe of Extreme Multi-Messenger Astrophysics
PUEO	Payload for Ultrahigh Energy Observations
RNO-G	Radio Neutrino Observatory in Greenland
SKA	Square Kilometer Array

[a] e-mail: frank.schroeder@kit.edu (corresponding author)

Published online: 28 February 2025

TAROGE	Taiwan Astroparticle Radiowave Observatory for Geo-synchrotron Emissions
TREND	Tianshan Radio Experiment for Neutrino Detection
Tunka-Rex	Tunka Radio Extension

1 Introduction

This article reviews the status and recent progress regarding the radio detection of extensive air showers—atmospheric particle cascades initiated by high energy cosmic particles. It complements my other reviews on this topic [1–3] and provides an updated overview of current and planned experiments featuring radio antennas for air-shower detections. For a more complete view of the topic including theory and the physics behind simulations of the radio signal, I also recommend reading reviews by other authors, such as [4, 5]. Particular emphasis in this review is given on recent experimental progress.

2 Radio emission of air showers

The radio signal of air showers is mostly generated by the electrons and positrons of the electromagnetic shower component and beamed in the forward direction. The emission is coherent, i.e., the amplitude of the radio signal scales approximately linearly and the power quadratically with the number of electromagnetic particles, which itself is approximately proportional to the energy of the primary particle [6]. The coherence conditions for the emission are optimal under the Cherenkov angle, which is of order 1° in air, where the radio emission extends to the highest frequencies of a few GHz [7]. As the shower front has a thickness of only a few meters, the radio emission is a short pulse, few ns to few 100s of ns, and has a broad frequency spectrum with typical experiments operating in a band somewhere between 30 MHz and a few GHz. Because the unavoidable galactic radio noise decreases with frequency, the frequency band has impact on the signal-to-noise ratio [8, 9]. Hence, the frequency band is an important aspect of the design of an antenna array and ideally is optimized for the science goals of an experiment.

The main mechanism of air-shower radio emission is the deflection of the electrons and positrons in the shower front by the Earth's magnetic field. This induces a time varying transverse current leading to radio emission linearly polarized in the $v \times B$ direction in the shower plane, where v is the shower axis and B the direction of the magnetic field. Therefore, the strength of the radio emission does not only depend on the zenith angle, but

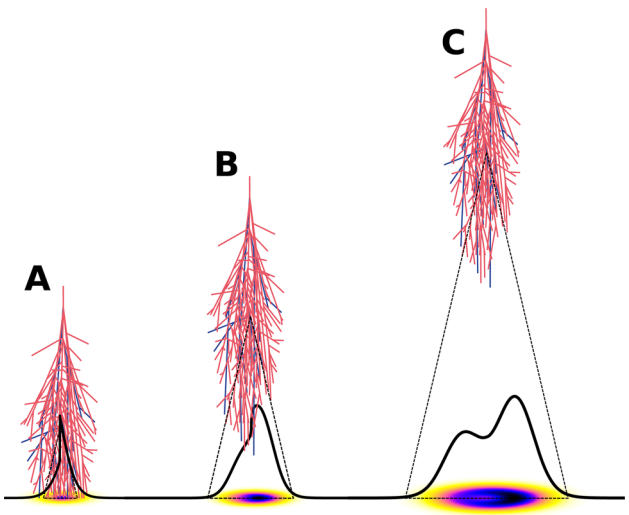

Fig. 1 Air showers with different depth of shower maximum (**A**–**C**, where **A** is closest to the ground) and the lateral distribution of the energy fluence of their radio emission illustrated in two ways: through the darkness of the color of the two-dimensional footprint and through the one-dimensional lateral distribution. The asymmetry is caused by interference of geomagnetic and Askaryan emission. The dip in the center is visible only for distant shower maxima and results from the emission being enhanced at the Cherenkov angle. Reprinted from [10] with permission from Elsevier

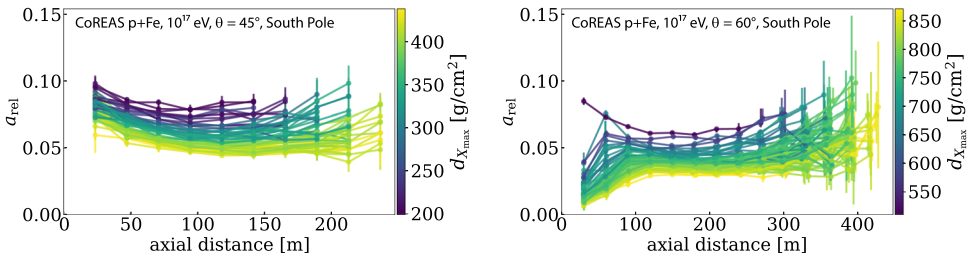

Fig. 2 Amplitude of the Askaryan emission A relative to the geomagnetic G emission for the ground level at the geographic South Pole for two different zenith angles as function of the distance from the shower axis and the distance to the shower maximum (determined with CoREAS simulations of the radio emission of air showers). The geomagnetic amplitude is corrected for the size of the geomagnetic Lorentz force with the plotted Askaryan fraction defined as $a_{\mathrm{rel}} = \frac{A}{G} \sin\alpha$, with α the angle between the Earth's magnetic field and the shower axis (Fig. modified from Ref. [24])

also on the azimuth angle of the air showers, which needs to be taken into account when modeling the aperture of radio arrays [11]. For very inclined showers and at high frequencies, the polarization pattern of geomagnetic emission becomes more synchrotron-like, which indicates that the curved tracks of the deflected electrons and positrons are important and not just the induction of the transverse current [12, 13]. Moreover, Askaryan emission due to the net charge excess in the shower front plays a small, but non-negligible role in air showers (see Fig. 2). Although it is an order of magnitude weaker than geomagnetic emission for most shower geometries, it interferes with geomagnetic emission, leading to an asymmetric lateral distribution of the radio signal on ground. Figure 1 illustrates that asymmetric radio footprint on ground and its dependence on the distance to the shower maximum. The size of the radio footprint can be as small as $100 - 200\,\mathrm{m}$ in diameter for vertical showers or extend over several 10 km for near-horizontal air showers [14].

When aiming at an accurate reconstruction of the air-shower direction, energy, and depth of maximum (X_{max}), several subtle effects need to be taken into account to achieve the best possible accuracy: for the direction, a plane-wave fit of the arrival times may achieve a resolution of $O(1^\circ)$, which is usually sufficient for cosmic-ray physics. Nonetheless, sub-degree resolution has been achieved when taking into account that the radio wavefront of air showers is approximately a hyperboloid [15, 16], which in some cases can be further approximated by a spherical or conical wavefront. For an accurate reconstruction of the energy of the air shower, the azimuthal asymmetry of the radio footprint on ground is important [6, 17, 18], and one needs to be aware that the radiation energy is a not a direct measure for the total shower energy, but proportional to the size of the electromagnetic shower component. Depending on the method used, such as interferometry [19, 20] or template fitting [21–23], the shape of the radio wavefront and the lateral distribution are also important for an accurate reconstruction of X_{max}.

3 Radio experiments for air showers

Radio pulses from air showers were first measured in the 1960s with analog experiments [25]. While these measurements were sufficient to confirm the main features of geomagnetic radio emission, the accuracy obtained for important air-shower observables, such as the energy and depth of shower maximum could not compete with other techniques. This changed only with digital radio arrays combined with computational pipelines for data analysis [26–28], including modern methods, such as template fitting [21, 22, 29, 30], and artificial neural networks [31–33]. Moreover, improved techniques for time [34, 35] and amplitude calibration [36, 37] of radio arrays have enabled a high data quality of current experiments. Finally, state-of-the-art Monte Carlo simulation codes, such as CoREAS [38] and ZHAireS [39], describe the radio emission in sufficient detail for an accurate interpretation of measured data.

LOPES [19] and CODALEMA [40] were a first generation of digital radio arrays, providing several proof-of-principles, such as for digital radio interferometry of air showers [41] and for the sensitivity of radio measurements to the longitudinal shower development [42]. AERA [30], LOFAR [44], TREND [45], and Tunka-Rex [18] belong to a second generation that demonstrated a precision for the reconstructed shower energy and X_{max} comparable to the established air-fluorescence and air-Cherenkov techniques [6, 21, 22, 30]. As enhancements of particle-detector arrays, radio detectors can thus enhance the measurement accuracy for the cosmic-ray energy and mass composition.

Nowadays, a third generation of digital radio experiments has started aiming at cosmic-ray science in the energy range above $10^{16}\,\mathrm{eV}$, with some experiments like the AugerPrime radio upgrade of the Pierre Auger Observatory under construction [46], and others planned, such as the IceCube-Gen2 surface array [47], with prototype stations in operation [23]. Following the example of LOFAR, also other antenna arrays built primarily for radio astronomy

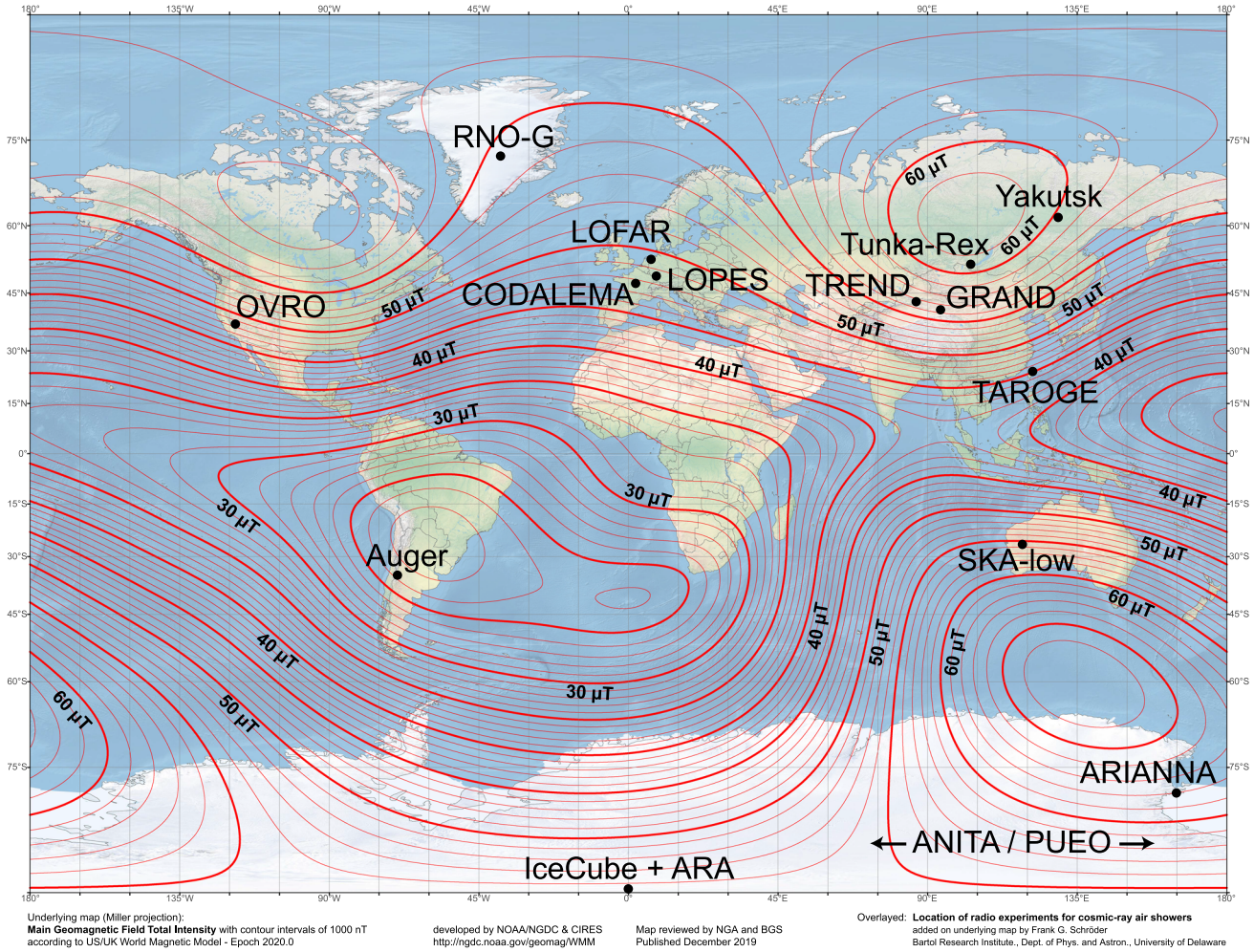

Fig. 3 Location of radio experiments for air-shower detection and the local strength of the geomagnetic field [see reference in the figure and in the text]

can also detect air showers in parallel to astronomical observations, in particular, OVRO [48] and the future SKA-low array [49]. Moreover, several experiments designed primarily to search for neutrino-induced radio signals also detected air showers, such as the ground-based radio arrays ARIANNA [50], RNO-G [51], TAROGE [52], BEACON [53], and GRAND (with its GRANDproto300 protoype array for cosmic-ray air showers) [54], and the balloon-borne radio probes ANITA [55], PUEO [56], and POEMMA Balloon Radio (PBR) [57].

Figure 3 and Table 1 provide an overview of the location and characteristics of several of these radio experiments for air-shower detection. A table with the abbreviated and full names of the experiments can be found at the beginning of this article (Caveat: In some cases, the full name does not reflect the later stages of the projects, e.g., because of additional locations or antenna types used.
).

Many of these radio arrays are triggered by other air-shower detectors, such as arrays of particle detectors, and share a common infrastructure for data taking. Self-triggering, which is required for stand-alone radio detection, has been demonstrated by several experiments [45, 48, 55, 58]. However, self-triggering increases the detection threshold compared to external air-shower triggers and is mostly important for radio detectors aiming at huge exposure for ultrahigh-energy neutrinos searches. For many cosmic-ray science goals, not only statistics, but also high accuracy is important, which is more easily achieved by hybrid detection of air showers with several techniques. Thus, an external trigger comes almost for free in air-shower arrays featuring coincident detection of air showers with particle detectors and radio antennas.

Table 1 Selected digital antenna arrays used for air-shower detection, and the values of the international geomagnetic reference model (IGRF) for the experimental site: the zenith angle of the geomagnetic field, $\theta_{\mathrm{geo}} = 90^\circ - |\mathrm{inclination}|$, and the magnetic field strength B_{geo}

Experiment or location	Latitude	Longitude	Altitude in m	θ_{geo} in °	B_{geo} in μ T	Number of antennas	Area in km^2	Band in MHz
LOPES	49°06′ N	8°26′ E	110	25.2°	48.1	30	0.04	40–80
Yakutsk	61°42′ N	129°24′ E	100	13.5°	59.9	6	0.1	32
CODALEMA	47°23′ N	2°12′ E	130	27.0°	47.5	60	1	2–200
TREND	42°56′ N	86°41′ E	2650	26.2°	56.1	50	1.2	50–100
Auger	35°06′ S	69°30′ W	1550	53.0°	23.5	153	17	30–80
LOFAR	52°55′ N	6°52′ E	5	22.0°	49.7	≈ 300	0.2	10–240
Tunka-Rex	51°49′ N	103°04′ E	675	18.0°	60.4	63	1	30–80
South Pole	90° S	–	2834	18.0°	54.4	Few	–	Various
ARIANNA	78°45′ S	165°00′ E	400	10.0°	62.1	32	5	50–1000
SKA-low	26°41′ S	116°38′ E	370	29.9°	55.6	60, 000	1	50–350
RNO-G	72°35′ N	38°28′ W	3216	18.9°	54.8	105	50	80–650
OVRO	37°14′ N	118°17′ W	1222	38.4°	48.0	256	0.04	30–80
TAROGE	24°17′ N	121°44′ E	1000	53.8°	45.2	4	–	180–350
BEACON	37°35′ N	118°14′ W	1180	38.1°	48.2	4	–	30–80
GRANDproto300	41° N	94° E	1300	37.9°	56.7	230	200	50–200

The numbers of antennas, the approximate areas covered with antennas, and the nominal frequency bands are given. However, many experiments were used also in configurations different from the one stated in the table or feature additional antennas for other purposes than air-shower detection, and many analyses are based on subsets of antennas and smaller sub-bands

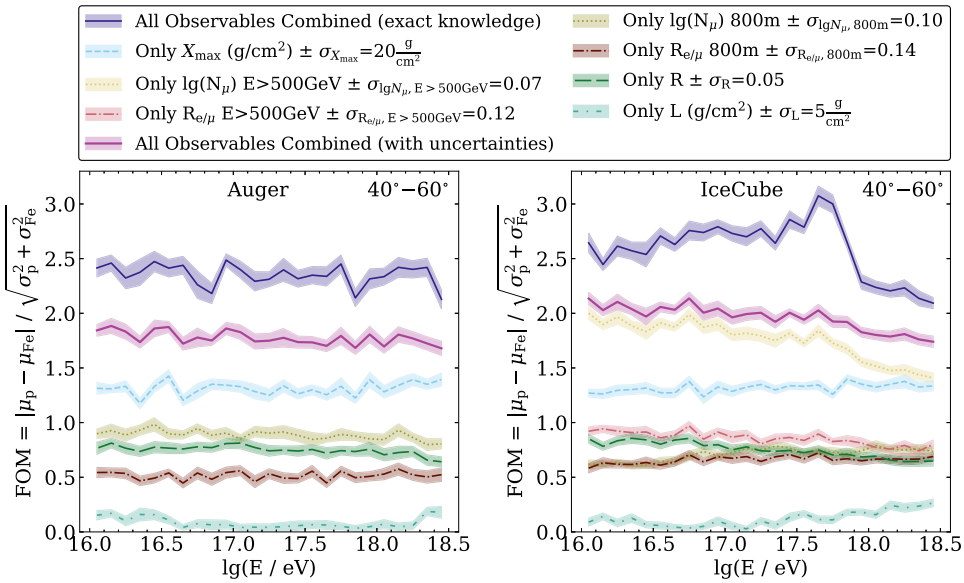

Fig. 4 Figure of merit (FOM) for the event-by-event sensitivity of various air-shower observables and their combination to separate air showers initiated by protons and iron nuclei. The results are for CORSIKA simulations with Sibyll 2.3c and 2.3d in the zenith angle range of $40^\circ - 60^\circ$ for the sites of the Pierre Auger Observatory and IceCube, respectively. X_{max} and the muon number N_μ provide the highest separation power, where muons for the Auger site are muons at 800 m axis distance at the surface and for IceCube high-energy muons as detectable by the deep detector. $R_{e/\mu}$ is the electron–muon ratio at ground. X_{max}, R, and L are parameters of the Gaisser–Hillas function describing the longitudinal shower profile. No detector simulation has been done, but some measurement uncertainties have been included as stated in the legend (figure modified from Ref. [59])

4 Future developments

Several future projects plan to use radio instrumentation, mostly to increase the accuracy of air-shower measurements. In particular, increasing the accuracy for the rigidity of cosmic-ray nuclei is important to search for the sources of the most energetic galactic and extragalactic cosmic rays through mass-sensitive anisotropy [60, 61]. In addition to an accurate energy determination, which can be provided by radio detectors, this primarily requires event-by-event mass sensitivity. Provided that the shower energy is known, the two most mass sensitive shower observables are the the depth of shower maximum, X_{max}, and the muon number N_{μ}. Therefore, air-shower arrays featuring both radio and muon detection are ideal for this purpose [59, 62].

In addition to further efforts to increase the accuracy of radio measurements through better calibration and analysis techniques, a number of new projects are planned for the next decade relying on radio detection, some of them making use of coincident shower measurements of radio and muon detectors:

IceCube-Gen2 [47] will continue a long tradition of cosmic-ray physics at the South Pole [63], as cosmic rays in the energy range of the galactic-to-extragalactic transition will complement the primary science case of neutrino astronomy. The surface array will feature scintillation panels and radio antennas for air showers [64], which in combination with high-energy muons measured by an optical array deep in the ice will provide high per-event mass sensitivity.

GCOS will consist of air-shower arrays at several sites, together increasing the exposure of current ultrahigh-energy cosmic-ray observatories by an order of magnitude and at the same time featuring per-event mass sensitivity [65]. At least one site will likely feature radio antennas, possibly for calibration or as enhancement of water-Cherenkov detectors following the concept of AugerPrime, the upgrade of the Pierre Auger Observatory. Among several other improvements of the Pierre Auger Observatory, such as new electronics and scintillation panels, a radio antenna has been added to each surface detector to provide a radio measurement of highly inclined air showers [46].

There are also science cases in cosmic-ray physics for future radio arrays without muon detectors. Examples are the huge exposure that can be provided by GRAND [54]. As GCOS, GRAND will feature several sites, with a total area even larger than GCOS. Although GRAND will be optimized for neutrino detection, it will also collect a huge statistics of ultrahigh-energy cosmic rays, and common sites between GRAND and GCOS can leverage synergies.

For the PeV-to-EeV energy range, SKA-low will provide the option to observe air showers in parallel to radio astronomy. The huge number of several 10, 000s of antennas will enable measuring the radio emission of air showers in unprecedented detail, including the shape parameters L and R for the width and asymmetry of the longitudinal shower profile, i.e., the number of particles as a function of atmospheric depth X:

$$N(X) = N_{\mathrm{max}}\left(1 + \frac{R(X - X_{\mathrm{max}})}{L}\right)^{R^{-2}} \exp\left(-\frac{X - X_{\mathrm{max}}}{LR}\right).$$

Fig. 5 Photos of SKALA v2 antennas used in prototype stations of the IceCube-Gen2 surface array at IceCube at the South Pole (left) and at the Pierre Auger Observatory in Argentina (right)

While L and R do not feature significant event-by-event mass separation power (cf. Fig. 4), they provide a novel approach to test hadronic interaction models and to statistically determine the proton and helium fractions among the primary cosmic-ray particles [66]. Last but not least, there are significant synergies among these experiments, e.g., the SKALA antennas developed for SKA-low [67] are also the reference design for the IceCube-Gen2 surface array, and prototype stations with SKALA v2 antennas have been deployed not only at the South Pole, but also at the Telescope Array and at the Pierre Auger Observatory (see Fig. 5).

5 Conclusion

Digital antenna arrays have been shown to feature an accuracy for the arrival direction, energy, and $X_{\max}$ competitive with established detection techniques for air showers. This achievement has been enabled by progress in the instrumentation and its calibration, an improved understanding of the radio emission of air showers, and by sophisticated computational analysis techniques. While progress on all of these aspects continues, the level achieved is already sufficient to make radio detection an essential technique for cosmic-ray physics of the coming decade. We are therefore seeing a number of experiments targeting both particle physics and astrophysics questions related to the most energetic galactic and extragalactic cosmic rays with the help of radio antennas.

Acknowledgements The author thanks the organizers of the Radio Neutrino and Cosmic Rays Astronomy Workshop for the opportunity to deliver a remote lecture on 19 April 2024. The research of the author is supported by several funding agencies: NASA EPSCoR award #80NSSC22M0222, U.S. National Science Foundation awards #2019597, #2046386, and #2209483, Sloan Research Foundation. This project has received funding from the European Research Council (ERC) under the European Union's Horizon 2020 research and innovation programme (Grant agreement No 802729). This research was supported in part through the use of Information Technologies (IT) resources at the University of Delaware, specifically the high-performance computing resources.

Funding Open Access funding enabled and organized by Projekt DEAL.

References

1. F.G. Schröder, Radio detection of cosmic-ray air showers and high-energy neutrinos. Prog. Part. Nucl. Phys. **93**, 1–68 (2017). https://doi.org/10.1016/j.ppnp.2016.12.002. arXiv:1607.08781 [astro-ph.IM]
2. F.G. Schröder, Digital antenna arrays for ultra-high-energy cosmic particles, in *Large Area Networked Detectors for Particle Astrophysics* (2022), pp. 59–91. https://doi.org/10.1142/9781800612617_0003
3. F.G. Schröder, Digital radio arrays for the detection of air showers initiated by ultra-high-energy particles. Acta Phys. Polon. Suppl. **15**(3), 3 (2022). https://doi.org/10.5506/APhysPolBSupp.15.3-A3. arXiv:2204.12631 [astro-ph.HE]
4. T. Huege, Radio detection of cosmic ray air showers in the digital era. Phys. Rep. **620**, 1–52 (2016). https://doi.org/10.1016/j.physrep.2016.02.001. arXiv:1601.07426 [astro-ph.IM]
5. J. Alvarez-Muñiz, E. Zas, Progress in the simulation and modelling of coherent radio pulses from ultra high-energy cosmic particles. Universe **8**(6), 297 (2022). https://doi.org/10.3390/universe8060297
6. A. Aab et al., Measurement of the radiation energy in the radio signal of extensive air showers as a universal estimator of cosmic-ray energy. Phys. Rev. Lett. **116**(24), 241101 (2016). https://doi.org/10.1103/PhysRevLett.116.241101. arXiv:1605.02564 [astro-ph.HE]
7. R. Šmída et al., First experimental characterization of microwave emission from cosmic ray air showers. Phys. Rev. Lett. **113**(22), 221101 (2014). https://doi.org/10.1103/PhysRevLett.113.221101. arXiv:1410.8291 [astro-ph.IM]
8. V.A. Balagopal, A. Haungs, T. Huege, F.G. Schröder, Search for PeVatrons at the Galactic Center using a radio air-shower array at the South Pole. Eur. Phys. J. C **78**(2), 111 (2018). [Erratum: Eur. Phys. J. C 78, 1017 (2018), Erratum: Eur.Phys.J.C 81, 483 (2021)]. https://doi.org/10.1140/epjc/s10052-018-5537-2. arXiv:1712.09042 [astro-ph.IM]
9. F.G. Schröder, A.L. Connolly, T. Huege, A. Rehman, Towards a standard definition of the signal-to-noise ratio for radio signals of ultra-high-energy particles. PoS **ARENA2022**, 027 (2023). https://doi.org/10.22323/1.424.0027. arXiv:2306.05901 [astro-ph.IM]

10. C. Glaser, S. Jong, M. Erdmann, J.R. Hörandel, An analytic description of the radio emission of air showers based on its emission mechanisms. Astropart. Phys. **104**, 64–77 (2019). https://doi.org/10.1016/j.astropartphys.2018.08.004. arXiv:1806.03620 [astro-ph.HE]
11. V. Lenok, F.G. Schröder, A probabilistic model for the efficiency of cosmic-ray radio arrays. JCAP **06**, 014 (2023). https://doi.org/10.1088/1475-7516/2023/06/014. arXiv:2208.07233 [astro-ph.IM]
12. C.W. James, Nature of radio-wave radiation from particle cascades. Phys. Rev. D **105**(2), 023014 (2022). https://doi.org/10.1103/PhysRevD.105.023014. arXiv:2201.01298 [astro-ph.HE]
13. S. Chiche, C. Zhang, F. Schlüter, K. Kotera, T. Huege, K.D. Vries, M. Tueros, M. Guelfand, Loss of coherence and change in emission physics for radio emission from ery inclined cosmic-ray air showers (2024). arXiv:2404.14541 [astro-ph.HE]
14. A. Aab et al., Observation of inclined EeV air showers with the radio detector of the Pierre Auger Observatory. JCAP **10**, 026 (2018). https://doi.org/10.1088/1475-7516/2018/10/026. arXiv:1806.05386 [astro-ph.IM]
15. W.D. Apel et al., The wavefront of the radio signal emitted by cosmic ray air showers. JCAP **09**, 025 (2014). https://doi.org/10.1088/1475-7516/2014/09/025. arXiv:1404.3283 [hep-ex]
16. A. Corstanje et al., The shape of the radio wavefront of extensive air showers as measured with LOFAR. Astropart. Phys. **61**, 22–31 (2015). https://doi.org/10.1016/j.astropartphys.2014.06.001. arXiv:1404.3907 [astro-ph.HE]
17. D. Kostunin, P.A. Bezyazeekov, R. Hiller, F.G. Schröder, V. Lenok, E. Levinson, Reconstruction of air-shower parameters for large-scale radio detectors using the lateral distribution. Astropart. Phys. **74**, 79–86 (2016). https://doi.org/10.1016/j.astropartphys.2015.10.004. arXiv:1504.05083 [astro-ph.HE]
18. P.A. Bezyazeekov et al., Radio measurements of the energy and the depth of the shower maximum of cosmic-ray air showers by Tunka-Rex. JCAP **01**, 052 (2016). https://doi.org/10.1088/1475-7516/2016/01/052. arXiv:1509.05652 [hep-ex]
19. W.D. Apel et al., Final results of the LOPES radio interferometer for cosmic-ray air showers. Eur. Phys. J. C **81**(2), 176 (2021). https://doi.org/10.1140/epjc/s10052-021-08912-4. arXiv:2102.03928 [astro-ph.HE]
20. H. Schoorlemmer, W.R. Carvalho, Radio interferometry applied to the observation of cosmic-ray induced extensive air showers. Eur. Phys. J. C **81**(12), 1120 (2021). https://doi.org/10.1140/epjc/s10052-021-09925-9. arXiv:2006.10348 [astro-ph.HE]
21. S. Buitink et al., Method for high precision reconstruction of air shower X_{max} using two-dimensional radio intensity profiles. Phys. Rev. D **90**(8), 082003 (2014). https://doi.org/10.1103/PhysRevD.90.082003. arXiv:1408.7001 [astro-ph.IM]
22. P.A. Bezyazeekov et al., Reconstruction of cosmic ray air showers with Tunka-Rex data using template fitting of radio pulses. Phys. Rev. D **97**(12), 122004 (2018). https://doi.org/10.1103/PhysRevD.97.122004. arXiv:1803.06862 [astro-ph.IM]
23. R. Turcotte-Tardif et al., Estimation of Xmax for air showers measured at IceCube with elevated radio antennas of a prototype surface station. PoS **ICRC2023**, 326 (2023). https://doi.org/10.22323/1.444.0326
24. E.N. Paudel, A. Coleman, F.G. Schröder, Simulation study of the relative Askaryan fraction at the South Pole. Phys. Rev. D **105**(10), 103006 (2022). https://doi.org/10.1103/PhysRevD.105.103006. arXiv:2201.03405 [hep-th]
25. H.R. Allan, Radio emission from extensive air showers. Prog. Elem. Part. Cosmic Ray Phys. **10**, 171 (1971)
26. P. Abreu et al., Advanced functionality for radio analysis in the offline software framework of the Pierre Auger Observatory. Nucl. Instrum. Methods A **635**, 92–102 (2011). https://doi.org/10.1016/j.nima.2011.01.049. arXiv:1101.4473 [astro-ph.IM]
27. C. Glaser, A. Nelles, I. Plaisier, C. Welling, S.W. Barwick, D. García-Fernández, G. Gaswint, R. Lahmann, C. Persichilli, NuRadioReco: a reconstruction framework for radio neutrino detectors. Eur. Phys. J. C **79**(6), 464 (2019). https://doi.org/10.1140/epjc/s10052-019-6971-5. arXiv:1903.07023 [astro-ph.IM]
28. R. Abbasi et al., Framework and tools for the simulation and analysis of the radio emission from air showers at IceCube. JINST **17**(06), 06026 (2022). https://doi.org/10.1088/1748-0221/17/06/P06026. arXiv:2205.02258 [astro-ph.HE]
29. A. Abdul Halim et al., Radio measurements of the depth of air-shower maximum at the Pierre Auger Observatory. Phys. Rev. D **109**(2), 022002 (2024). https://doi.org/10.1103/PhysRevD.109.022002. arXiv:2310.19966 [astro-ph.HE]
30. A. Abdul Halim et al., Demonstrating agreement between radio and fluorescence measurements of the depth of maximum of extensive air showers at the Pierre Auger Observatory. Phys. Rev. Lett. **132**(2), 021001 (2024). https://doi.org/10.1103/PhysRevLett.132.021001. arXiv:2310.19963 [astro-ph.HE]
31. M. Erdmann, F. Schlüter, R. Smida, Classification and recovery of radio signals from cosmic ray induced air showers with deep learning. JINST **14**(04), 04005 (2019). https://doi.org/10.1088/1748-0221/14/04/P04005. arXiv:1901.04079 [astro-ph.IM]
32. P. Bezyazeekov et al., Reconstruction of sub-threshold events of cosmic-ray radio detectors using an autoencoder. PoS **ICRC2021**, 223 (2021). https://doi.org/10.22323/1.395.0223. arXiv:2108.04627 [astro-ph.IM]
33. A. Rehman, A. Coleman, F.G. Schröder, Deep Learning for the classification and recovery of cosmic-ray signals against background measured at South Pole. PoS **ARENA2022**, 012 (2023). https://doi.org/10.22323/1.424.0012
34. F.G. Schroder et al., New method for the time calibration of an interferometric radio antenna array. Nucl. Instrum. Methods A **615**, 277–284 (2010). https://doi.org/10.1016/j.nima.2010.01.072. arXiv:1002.3775 [astro-ph.IM]
35. A. Aab et al., Nanosecond-level time synchronization of autonomous radio detector stations for extensive air showers. JINST **11**(01), 01018 (2016). https://doi.org/10.1088/1748-0221/11/01/P01018. arXiv:1512.02216 [physics.ins-det]

36. W.D. Apel et al., Improved absolute calibration of LOPES measurements and its impact on the comparison with REAS 3.11 and CoREAS simulations. Astropart. Phys. **75**, 72–74 (2016). https://doi.org/10.1016/j.astropartphys.2015.09.002. arXiv:1507.07389 [astro-ph.HE]
37. A. Aab et al., Calibration of the logarithmic-periodic dipole antenna (LPDA) radio stations at the Pierre Auger Observatory using an octocopter. JINST **12**(10), 10005 (2017). https://doi.org/10.1088/1748-0221/12/10/T10005. arXiv:1702.01392 [astro-ph.IM]
38. T. Huege, M. Ludwig, C.W. James, Simulating radio emission from air showers with CoREAS. AIP Conf. Proc. **1535**(1), 128 (2013). https://doi.org/10.1063/1.4807534. arXiv:1301.2132 [astro-ph.HE]
39. J. Alvarez-Muniz, W.R. Carvalho Jr., E. Zas, Monte Carlo simulations of radio pulses in atmospheric showers using ZHAireS. Astropart. Phys. **35**, 325–341 (2012). https://doi.org/10.1016/j.astropartphys.2011.10.005. arXiv:1107.1189 [astro-ph.HE]
40. D. Ardouin et al., Radio-detection signature of high energy cosmic rays by the CODALEMA Experiment. Nucl. Instrum. Methods A **555**, 148 (2005). https://doi.org/10.1016/j.nima.2005.08.096. arXiv:astro-ph/0504297
41. H. Falcke et al., Detection and imaging of atmospheric radio flashes from cosmic ray air showers. Nature **435**, 313–316 (2005). https://doi.org/10.1038/nature03614. arXiv:astro-ph/0505383
42. W.D. Apel et al., Experimental evidence for the sensitivity of the air-shower radio signal to the longitudinal shower development. Phys. Rev. D **85**, 071101 (2012). https://doi.org/10.1103/PhysRevD.85.071101. arXiv:1203.3971 [astro-ph.IM]
43. I.S. Petrov, S.P. Knurenko, Study of cosmic rays with energies above 5 EeV using radio method. Phys. Atom. Nucl. **87**(2), 77–85 (2024). https://doi.org/10.1134/S1063778824020157
44. P. Schellart et al., Detecting cosmic rays with the LOFAR radio telescope. Astron. Astrophys. **560**, 98 (2013). https://doi.org/10.1051/0004-6361/201322683. arXiv:1311.1399 [astro-ph.IM]
45. D. Ardouin et al., First detection of extensive air showers by the TREND self-triggering radio experiment. Astropart. Phys. **34**, 717–731 (2011). https://doi.org/10.1016/j.astropartphys.2011.01.002. arXiv:1007.4359 [astro-ph.IM]
46. A. AbdulHalim et al., Status and expected performance of the AugerPrime Radio Detector. PoS **ICRC2023**, 344 (2023). https://doi.org/10.22323/1.444.0344
47. R. Abbasi et al., IceCube-Gen2 Technical Design Report (TDR). IceCube-Gen2 Website (2024). https://icecube-gen2.wisc.edu/science/publications/tdr/. Accessed 10 Feb 2025
48. R. Monroe et al., Self-triggered radio detection and identification of cosmic air showers with the OVRO-LWA. Nucl. Instrum. Methods A **953**, 163086 (2020). https://doi.org/10.1016/j.nima.2019.163086. arXiv:1907.10193 [astro-ph.IM]
49. S. Buitink et al., High-resolution air shower observations with the Square Kilometer Array. PoS **ICRC2023**, 503 (2023). https://doi.org/10.22323/1.444.0503
50. S.W. Barwick et al., Radio detection of air showers with the ARIANNA experiment on the Ross Ice Shelf. Astropart. Phys. **90**, 50–68 (2017). https://doi.org/10.1016/j.astropartphys.2017.02.003. arXiv:1612.04473 [astro-ph.IM]
51. J.A. Aguilar et al.: Design and sensitivity of the Radio Neutrino Observatory in Greenland (RNO-G). JINST **16**(03), 03025 (2021). https://doi.org/10.1088/1748-0221/16/03/P03025. arXiv:2010.12279 [astro-ph.IM]. [Erratum: JINST 18, E03001 (2023)]
52. S.-H. Wang et al., TAROGE-M: radio antenna array on antarctic high mountain for detecting near-horizontal ultra-high energy air showers. JCAP **11**, 022 (2022). https://doi.org/10.1088/1475-7516/2022/11/022. arXiv:2207.10616 [astro-ph.HE]
53. A. Zeolla et al., Detection of radio emission by cosmic rays with the BEACON prototype. PoS **ICRC2023**, 1019 (2023). https://doi.org/10.22323/1.444.1019
54. J. Álvarez-Muñiz et al., The Giant Radio Array for Neutrino Detection (GRAND): science and design. Sci. China Phys. Mech. Astron. **63**(1), 219501 (2020). https://doi.org/10.1007/s11433-018-9385-7. arXiv:1810.09994 [astro-ph.HE]
55. S. Hoover et al., Observation of ultra-high-energy cosmic rays with the ANITA balloon-borne radio interferometer. Phys. Rev. Lett. **105**, 151101 (2010). https://doi.org/10.1103/PhysRevLett.105.151101. arXiv:1005.0035 [astro-ph.HE]
56. Q. Abarr et al., The Payload for Ultrahigh Energy Observations (PUEO): a white paper. JINST **16**(08), 08035 (2021). https://doi.org/10.1088/1748-0221/16/08/P08035. arXiv:2010.02892 [astro-ph.IM]
57. M. Battisti, J. Eser, A. Olinto, G. Osteria, Poemma-balloon with radio: a balloon-born multi-messenger multi-detector observatory. Nuclear Instrum. Methods Phys. Res. Sect. A Accelerators Spectrom. Detect. Assoc. Equip. (2024). https://doi.org/10.1016/j.nima.2024.169819
58. P. Abreu et al., Results of a self-triggered prototype system for radio-detection of extensive air showers at the Pierre Auger Observatory. JINST **7**, 11023 (2012). https://doi.org/10.1088/1748-0221/7/11/P11023. arXiv:1211.0572 [astro-ph.HE]
59. B. Flaggs, A. Coleman, F.G. Schröder, Studying the mass sensitivity of air-shower observables using simulated cosmic rays. Phys. Rev. D **109**(4), 042002 (2024). https://doi.org/10.1103/PhysRevD.109.042002. arXiv:2306.13246 [hep-ph]
60. F.G. Schröder et al., High-energy galactic cosmic rays (Astro2020 science white paper). Bull. Am. Astron. Soc. **51**, 131 (2019). arXiv:1903.07713 [astro-ph.HE]
61. A. Coleman et al., Ultra high energy cosmic rays—the intersection of the cosmic and energy frontiers. Astropart. Phys. **149**, 102819 (2023). https://doi.org/10.1016/j.astropartphys.2023.102819. arXiv:2205.05845 [astro-ph.HE]
62. E.M. Holt, F.G. Schröder, A. Haungs, Enhancing the cosmic-ray mass sensitivity of air-shower arrays by combining radio and muon detectors. Eur. Phys. J. C **79**(5), 371 (2019). https://doi.org/10.1140/epjc/s10052-019-6859-4. arXiv:1905.01409 [astro-ph.HE]

63. D. Soldin, P.A. Evenson, H. Kolanoski, A.A. Watson, Cosmic-ray physics at the South Pole. Astropart. Phys. **161**, 102992 (2024). https://doi.org/10.1016/j.astropartphys.2024.102992. arXiv:2311.14474 [astro-ph.HE]
64. F.G. Schröder, Design and expected performance of the IceCube-Gen2 surface array and its radio component. PoS **ARENA2022**, 058 (2023). https://doi.org/10.22323/1.424.0058. arXiv:2306.05900 [astro-ph.HE]
65. R. Alves Batista, Science with the Global Cosmic-ray Observatory (GCOS). PoS **ICRC2023**, 281 (2023). https://doi.org/10.22323/1.444.0281. arXiv:2309.17324 [astro-ph.HE]
66. S. Buitink et al., Performance of SKA as an air shower observatory. PoS **ICRC2021**, 415 (2021). https://doi.org/10.22323/1.395.0415
67. E. de Lera Acedo, N. Drought, B. Wakley, A. Faulkner, Evolution of SKALA (SKALA-2), the log-periodic array antenna for the SKA-low instrument, in *2015 International Conference on Electromagnetics in Advanced Applications (ICEAA)* (2015), pp. 839–843. https://doi.org/10.1109/ICEAA.2015.7297231